Anal. Chem. **2010,** *82,* 9058–9065

Hand-held Spectroscopic Device for In Vivo and Intraoperative Tumor Detection: Contrast Enhancement, Detection Sensitivity, and Tissue Penetration

Aaron M. Mohs,[†] Michael C. Mancini,[†] Sunil Singhal,[‡] James M. Provenzale,[§,||] Brian Leyland-Jones,[⊥] May D. Wang,[#] and Shuming Nie*[,†]

Department of Biomedical Engineering and Chemistry, Emory University and Georgia Institute of Technology, 101 Woodruff Circle Suite 2007, Atlanta, Georgia 30322, United States, Division of Thoracic Surgery, University of Pennsylvania School of Medicine, Philadelphia, Pennsylvania 19104, United States, Departments of Biomedical Engineering, Oncology and Radiology, Emory University, 101 Woodruff Circle, Suite 2007, Atlanta, Georgia 30322, United States, Department of Radiology, Duke University Medical Center, Durham, North Carolina 27710, United States, Department of Hematology and Medical Oncology, Emory University School of Medicine, Atlanta, Georgia 30322, United States, and Department of Biomedical Engineering, Georgia Institute of Technology, 313 Ferst Drive, UA Whitaker Building 4106, Atlanta, Georgia 30332, United States

Surgery is one of the most effective and widely used procedures in treating human cancers, but a major problem is that the surgeon often fails to remove the entire tumor, leaving behind tumor-positive margins, metastatic lymph nodes, and/or satellite tumor nodules. Here we report the use of a hand-held spectroscopic pen device (termed SpectroPen) and near-infrared contrast agents for intraoperative detection of malignant tumors, based on wavelength-resolved measurements of fluorescence and surface-enhanced Raman scattering (SERS) signals. The SpectroPen utilizes a near-infrared diode laser (emitting at 785 nm) coupled to a compact head unit for light excitation and collection. This pen-shaped device effectively removes silica Raman peaks from the fiber optics and attenuates the reflected excitation light, allowing sensitive analysis of both fluorescence and Raman signals. Its overall performance has been evaluated by using a fluorescent contrast agent (indocyanine green, or ICG) as well as a surface-enhanced Raman scattering (SERS) contrast agent (pegylated colloidal gold). Under in vitro conditions, the detection limits are approximately $2-5 \times 10^{-11}$ M for the indocyanine dye and $0.5-1 \times 10^{-13}$ M for the SERS contrast agent. Ex vivo tissue penetration data show attenuated but resolvable fluorescence and Raman signals when the contrast agents are buried 5−10 mm deep in fresh animal tissues. In vivo studies using mice bearing bioluminescent 4T1 breast tumors further demonstrate that the tumor borders can be precisely detected preoperatively and intraoperatively, and that the contrast signals are strongly correlated with tumor bioluminescence. After surgery, the SpectroPen device permits further evaluation of both positive and negative tumor margins around the surgical cavity, raising new possibilities for real-time tumor detection and image-guided surgery.

Most human cancers are treated by surgical resection, chemotherapy, and/or radiation. Surgery provides significant survival advantages for a broad range of tumor types, and cures approximately 45% of all patients with solid tumors.[1] To successfully treat a patient with surgery, the surgeon must remove the entire tumor at the time of surgery including the primary tumor, draining lymph nodes that may contain tumor cells, and small adjacent satellite nodules. Statistical data indicate that complete resection is the single most important predictor of patient survival for almost all solid tumors.[2] In lung, breast, prostate, colon, and pancreatic cancers, a complete resection has a three to 5-fold improvement in survival compared to partial resection.[3−8]

Recent advances in computed tomography (CT), positron emission tomography (PET), and hybrid techniques (such as CT/PET) have greatly improved tumor detection and surgical

* To whom correspondence should be addressed. E-mail: snie@emory.edu.
[†] Emory University and Georgia Institute of Technology.
[‡] University of Pennsylvania School of Medicine.
[§] Emory University.
[||] Duke University Medical Center.
[⊥] Emory University School of Medicine.
[#] Georgia Institute of Technology.

(1) De Grand, A. M.; Frangioni, J. V. *Technol. Cancer. Res. Treat.* **2003**, *2*, 553–562.
(2) Gebitekin, C.; Gupta, N. K.; Satur, C. M.; Olgac, G.; Martin, P. G.; Saunders, N. R.; Walker, D. R. *Eur. J. Cardiothorac. Surg.* **1994**, *8*, 339–342, discussion 342,334.
(3) Meric, F.; Mirza, N. Q.; Vlastos, G.; Buchholz, T. A.; Kuerer, H. M.; Babiera, G. V.; Singletary, S. E.; Ross, M. I.; Ames, F. C.; Feig, B. W.; Krishnamurthy, S.; Perkins, G. H.; McNeese, M. D.; Strom, E. A.; Valero, V.; Hunt, K. K. *Cancer* **2003**, *97*, 926–933.
(4) Karakiewicz, P. I.; Eastham, J. A.; Graefen, M.; Cagiannos, I.; Stricker, P. D.; Klein, E.; Cangiano, T.; Schroder, F. H.; Scardino, P. T.; Kattan, M. W. *Urology* **2005**, *66*, 1245–1250.
(5) Kuvshinoff, B.; Maghfoor, I.; Miedema, B.; Bryer, M.; Westgate, S.; Wilkes, J.; Ota, D. *Ann. Surg. Oncol.* **2001**, *8*, 163–169.
(6) Sienel, W.; Stremmel, C.; Kirschbaum, A.; Hinterberger, L.; Stoelben, E.; Hasse, J.; Passlick, B. *Eur. J. Cardiothorac. Surg.* **2007**, *31*, 522–527, discussion 527−528.
(7) Karni, T.; Pappo, I.; Sandbank, J.; Lavon, O.; Kent, V.; Spector, R.; Morgenstern, S.; Lelcuk, S. *Am. J. Surg.* **2007**, *194*, 467–473.

10.1021/ac102058k
Published on Web 10/06/2010

planning,[9,10] but these modalities do not provide real-time intraoperative assistance. Intraoperative magnetic resonance imaging (MRI) can assist in surgical resection of tumors, but it is time-consuming and substantially adds to the length of surgery, anesthesia time, and financial costs.[11] Intraoperative sonography has also shown promise for detection of breast cancer but has limited sensitivity for detection of masses less than 5 mm.[12] Faced with these difficulties, optical technologies based on cellular imaging, native fluorescence, and Raman scattering have gained considerable attention for tumor detection and diagnosis.[13−17] In particular, the level of autofluorescence from collagen, nicotinamide adenine dinucleotide (NADH), and flavin adenine dinucleotide (FAD) has been associated with malignancy in head and neck cancer.[17−19] Chemical and biochemical changes have been measured by laser Raman spectroscopy for margin assessment of breast cancer[15,20] and for noninvasive detection of cervical dysplasia during routine pelvic exams.[21] The underlying hypothesis is that small changes in cellular biochemistry could translate into spectroscopic differences that are measurable with fluorescence or Raman scattering. However, tumors are highly heterogeneous in their molecular and cellular compositions,[22] and biochemical differences in malignant and benign tissues are subject to natural variations in patient physiology and pathology.[23] Thus, autofluorescence and intrinsic Raman measurements often lead to unacceptable false-positive rates for benign tissues and unacceptable false-negative rates for malignant tissues.[24,25]

In this work, we have developed a hand-held spectroscopic pen device (called SpectroPen) and have utilized exogenous contrast agents for in vivo and intraoperative cancer detection. Due to tissue scattering and blood absorption, optical methods have relatively limited penetration depths.[26,27] For intraoperative applications, however, the lesions are surgically exposed and can be brought in close proximity to the imaging device, so they become accessible to optical illumination and detection. A problem in using exogenous contrast agents is that they are often unable to deeply penetrate solid tumors, especially when macromolecules such as monoclonal antibodies or nanoparticles are used.[28−30] For detection of tumor margins during surgery, on the other hand, the agents are detected at the tumor periphery and deep penetration is not required. Similarly, for detection of small and residual tumors, deep penetration is not required because small tumors do not have a high intratumoral pressure or a necrotic/hypoxic core, two factors in limiting tumor penetration of imaging and therapeutic agents.[28−30]

As discussed in detail below, we have evaluated the performance of the SpectroPen device by using both a fluorescent contrast agent (indocyanine green or ICG) and a surface-enhanced Raman scattering (SERS) contrast agent (pegylated colloidal gold). Under in vitro conditions, the hand-held device provides a detection limit of $2-5 \times 10^{-11}$ M for ICG and a detection limit of $0.5-1 \times 10^{-13}$ M for SERS. The tissue penetration depth is estimated to be about 5−10 mm depending on the tissue's optical properties and the ability to resolve contrast agent signals. We have also carried out in vivo studies using mice bearing bioluminescent 4T1 breast tumors. The results show that tumor margins could be precisely detected preoperatively and intraoperatively, and that the contrast signals are strongly correlated with the tumor's bioluminescence. After surgery, the SpectroPen device permits further evaluation of both positive and negative tumor margins around the surgical cavity.

It is also important to note that previous work has developed various compact fiberoptic devices for fluorescence and Raman measurements,[31−33] but has not examined their suitability for measuring exogenous contrast agents during surgical procedures. In this work, we have constructed an integrated fiber-optic spectroscopic system that is stably aligned and calibrated and is thus well suited for robust surgical use. A key insight for this design is that a rigid pen-sized fiberoptic unit can be used by a surgeon as a hand-held device to detect small tumors and other lesions in real time during surgery. To address the issue of tumor heterogeneity, we demonstrate that this spectroscopic system can

(8) Neoptolemos, J. P.; Stocken, D. D.; Dunn, J. A.; Almond, J.; Beger, H. G.; Pederzoli, P.; Bassi, C.; Dervenis, C.; Fernandez-Cruz, L.; Lacaine, F.; Buckels, J.; Deakin, M.; Adab, F. A.; Sutton, R.; Imrie, C.; Ihse, I.; Tihanyi, T.; Olah, A.; Pedrazzoli, S.; Spooner, D.; Kerr, D. J.; Friess, H.; Buchler, M. W. *Ann. Surg.* **2001**, *234*, 758–768.

(9) Gambhir, S. S. *Nat. Rev. Cancer* **2002**, *2*, 683–693.

(10) Townsend, D. W. *J. Nucl. Med.* **2001**, *42*, 533–534.

(11) Ramina, R.; Coelho Neto, M.; Giacomelli, A.; Barros, E., Jr.; Vosgerau, R.; Nascimento, A.; Coelho, G. *Acta Neurochir* **2010**, *152*, 27–33.

(12) Ngo, C.; Pollet, A. G.; Laperrelle, J.; Ackerman, G.; Gomme, S.; Thibault, F.; Fourchotte, V.; Salmon, R. J. *Ann. Surg. Oncol.* **2007**, *14*, 2485–2489.

(13) Dacosta, R. S.; Wilson, B. C.; Marcon, N. E. *Best Pract. Res., Clin. Gastroenterol.* **2006**, *20*, 41–57.

(14) Draga, R. O.; Grimbergen, M. C.; Vijverberg, P. L.; Swol, C. F.; Jonges, T. G.; Kummer, J. A.; Ruud Bosch, J. L. *Anal. Chem.* **2010**, *82*, 5993–5999.

(15) Haka, A. S.; Volynskaya, Z.; Gardecki, J. A.; Nazemi, J.; Lyons, J.; Hicks, D.; Fitzmaurice, M.; Dasari, R. R.; Crowe, J. P.; Feld, M. S. *Cancer Res.* **2006**, *66*, 3317–3322.

(16) Mo, J.; Zheng, W.; Low, J. J. H.; Ng, J.; Ilancheran, A.; Huang, Z. *Anal. Chem.* **2009**, *81*, 8908–8915.

(17) Schwarz, R. A.; Gao, W.; Redden Weber, C.; Kurachi, C.; Lee, J. J.; El-Naggar, A. K.; Richards-Kortum, R.; Gillenwater, A. M. *Cancer* **2009**, *115*, 1669–1679.

(18) Muller, M. G.; Valdez, T. A.; Georgakoudi, I.; Backman, V.; Fuentes, C.; Kabani, S.; Laver, N.; Wang, Z.; Boone, C. W.; Dasari, R. R.; Shapshay, S. M.; Feld, M. S. *Cancer* **2003**, *97*, 1681–1692.

(19) de Veld, D. C.; Skurichina, M.; Witjes, M. J.; Duin, R. P.; Sterenborg, H. J.; Roodenburg, J. L. *J. Biomed. Opt.* **2004**, *9*, 940–950.

(20) Haka, A. S.; Shafer-Peltier, K. E.; Fitzmaurice, M.; Crowe, J.; Dasari, R. R.; Feld, M. S. *Proc. Natl. Acad. Sci. U. S. A.* **2005**, *102*, 12371–12376.

(21) Kanter, E. M.; Vargis, E.; Majumder, S.; Keller, M. D.; Woeste, E.; Rao, G. G.; Mahadevan-Jansen, A. *J. Biophoton.* **2009**, *2*, 81–90.

(22) Liu, J.; Lau, S. K.; Varma, V. A.; Moffitt, R. A.; Caldwell, M.; Liu, T.; Young, A. N.; Petros, J. A.; Osunkoya, A. O.; Krogstad, T.; Leyland-Jones, B.; Wang, M. D.; Nie, S. *ACS Nano* **2010**, *4*, 2755–2765.

(23) Kanter, E. M.; Majumder, S.; Kanter, G. J.; Woeste, E. M.; Mahadevan-Jansen, A. *Am. J. Obstet. Gynecol.* **2009**, *200*, 512.e1−5.

(24) Ramanujam, N.; Mitchell, M. F.; Mahadevan-Jansen, A.; Thomsen, S. L.; Staerkel, G.; Malpica, A.; Wright, T.; Atkinson, N.; Richards-Kortum, R. *Photochem. Photobiol.* **1996**, *64*, 720–735.

(25) Schomacker, K. T.; Frisoli, J. K.; Compton, C. C.; Flotte, T. J.; Richter, J. M.; Nishioka, N. S.; Deutsch, T. F. *Lasers Surg. Med.* **1992**, *12*, 63–78.

(26) Qian, X.; Peng, X.-H.; Ansari, D. O.; Yin-Goen, Q.; Chen, G. Z.; Shin, D. M.; Yang, L.; Young, A. N.; Wang, M. D.; Nie, S. *Nat. Biotechnol.* **2008**, *26*, 83–90.

(27) Gao, X.; Cui, Y.; Levenson, R. M.; Chung, L. W. K.; Nie, S. *Nat. Biotechnol.* **2004**, *22*, 969–976.

(28) Jain, R. K. *Annu. Rev. Biomed. Eng.* **1999**, *1*, 241–263.

(29) Minchinton, A. I.; Tannock, I. F. *Nat. Rev. Cancer* **2006**, *6*, 583–592.

(30) Dreher, M. R.; Liu, W.; Michelich, C. R.; Dewhirst, M. W.; Yuan, F.; Chilkoti, A. *J. Natl. Cancer Inst.* **2006**, *98*, 335–344.

(31) Carrabba, M. M.; Spencer, K. M.; Rauh, R. D. *Proc. SPIE* **1991**, *1434*, 127–134.

(32) Christesen, S.; MacIver, B.; Process, L.; Sorrick, D.; Carrabba, M. M.; Bello, *J. Appl. Spectrosc.* **1999**, *53*, 850–855.

(33) Angel, S. M.; Myrick, M. L.; Vess, T. M. *Proc. SPIE* **1991**, *1534*, 72, doi: 10.1117/12.44232.

be combined with injected contrast agents for intraoperative cancer detection and tumor margin delineation. As a result, we have achieved much higher detection sensitivity and more consistent tumor signals than previous studies that relied on native fluorescence or normal Raman scattering.

EXPERIMENTAL SECTION

Reagents. Ultrapure water (18.2 MΩ) was used throughout this work. Indocyanine green (ICG), 3,3′-diethylthiatricarbocyanine iodide (DTTC), 2,2,2 tribromoethanol, tertiary amyl alcohol, and bovine serum albumin (BSA, 98%) were purchased from Sigma-Aldrich (St. Louis, MO). Citrate-stabilized gold colloids (60 nm diameter) at a concentration of 2.6×10^{10} particles/mL were obtained from Ted Pella, Inc. (Redding, CA). Dulbecco's Modified Eagle's Medium (DMEM) (4.5 g/L glucose, 4.00 mM L-glutamine), fetal bovine serum (FBS), antibiotic/antimycotic solution, and phosphate buffered saline (PBS) were purchased from Thermo Scientific HyClone (Logan, UT). XenoLight RediJect D-luciferin subtrate was purchased from Caliper Life Sciences (Hopkinton, MA). All reagents were used as purchased without further purification.

SpectroPen. A RamanProbe sampling head and connecting fiber optics were purchased from InPhotonics (Norwood, MA). The cylindrical stainless steel sampling head (diameter = 1.3 mm, length = 10 cm) was integrated with a 5 m two-fiber cable, one for laser excitation and the other for light collection. The sampling head and fiber cable were coupled via an FC connector to a spectrometer designed by Delta Nu (Laramie, WY). The combined sampling head and spectrometer system has a wavelength range of 800−930 nm with 0.6 nm spectral resolution for fluorescence measurement, and a Raman shift range of 200−2000 cm^{-1} with 8 cm^{-1} resolution for Raman measurement. Laser excitation was provided by a continuous-wave 200 mW diode laser emitting at 785 nm.

The SpectroPen was compared to a standard Raman spectrometer (Inspector, 785 nm excitation, 120 mW laser power, 0.6 nm resolution) (DeltaNu, Laramie, WY) to check for wavenumber accuracy across the entire spectral range. A Raman scattering spectra from polystyrene was acquired over 5 s from both the SpectroPen and the commercial Raman spectrometer to determine the spectral accuracy of the hand-held device. The sensitivity of the SpectroPen to detect ICG and SERS contrast agents was also determined. ICG was diluted in BSA solution to concentrations ranging from 25 nM to 50 pM. SERS nanoparticles were diluted in Milli-Q water to a concentration of 0.2−37.6 pM. Nanoparticle solutions of different concentrations were transferred (200 μL) into 96 well half-volume black microplates. The SpectroPen was fixed 10-mm above and centered over each well of the microplate. Signal collection times for each concentration ranged from 0.1 to 10 s. The relationship between the integrated signal intensity and the contrast agent concentration was statically analyzed with a linear regression model including calculated 95% confidence intervals. All statistical analyses were performed using Origin 6.1 software.

Nanoparticle Contrast Agents. Stock ICG solution was first dissolved in DMSO, and then diluted in aqueous solution containing the albumin protein (40 mg/mL, similar to the blood protein concentration). Under this condition, the ICG molecules quickly bound to albumin molecules, resulting in ICG-albumin complexes with a hydrodynamic size of 4−6 nm (diameter). The use of albumin also prevented ICG aggregation and fluorescence quenching.[34] Spectrally encoded and PEG-stabilized SERS nanoparticles were prepared according to Qian, Nie, and co-workers.[26] Briefly, aqueous diethylthiatricarbocyanine (DTTC) solution (4 μM) was added dropwise to a gold nanoparticle solution. The optimal SERS signals were detected when approximately 2×10^4 DTTC molecules were bound to each 60-nm gold particle. The particles were stabilized by the addition of a thiol-PEG solution (10 μM) and then purified by centrifugation.

Tissue Penetration Depth Measurement. Porcine tissues used for ex vivo studies were obtained from the Animal and Dairy Science Department at the University of Georgia (Athens, GA). Fluorescence and Raman spectra of porcine fat, liver, and lung were collected over 5−10 s. These tissues were chosen for both their relevance to disease processes and for their optical properties. To determine the depth at which the SpectroPen can detect fluorescent dyes or SERS nanoparticles in various organs, an 8 mm^3 section of the tissue was loaded with 20 μL of either 650 nM ICG or 300 pM SERS nanoparticle solution. Next, thinly sliced sections of the corresponding tissues were laid on top of the contrast-agent loaded specimen. After each tissue section was applied, fluorescent or Raman spectra were collected over 0.1 − 10 s with the SpectroPen. A distance of 1-cm was maintained between the SpectroPen tip and the top tissue layer, in order to simulate the SpectroPen position during surgical use. A layer of plastic wrap was placed in between the contrast-agent loaded tissue and subsequent tissue layers to prevent diffusion of contrast agents into the unlabeled tissue slices. Spectra were scaled as necessary to correct for different integration times and then integrated to obtain the reported signal intensity.

In Vivo and Intraoperative Measurements. All in vivo murine studies were performed under an approved protocol by the Emory University IACUC. The mouse mammary carcinoma cell line 4T1, which stably expresses a firefly luciferase gene, was obtained from Dr. Lily Yang at Emory University (Atlanta, GA). 4T1 cells were cultured in DMEM containing 10% FBS and 1X antibiotic/antimycotic agent. Prior to injection into mice, the cells were washed two times with PBS and diluted in sterile PBS to a final concentration of 2×10^7 cells/mL. Mammary tumors were inoculated into nude mice by the subcutaneous administration of 2×10^6 4T1 cells into the mouse flank. Once the tumors were approximately 4 mm in diameter, ICG was administered intravenously (i.v.) via a tail vein at a dose of 357 μg/kg. After 24 h, mice were anesthetized by intraperitoneal (i.p.) injection of a 2.5% solution of tribromoethanol (350 mg/kg). Tumor-bearing mice undergoing bioluminescence imaging were administered i.p. 100 uL of a luciferin solution (30 mg/mL). Bioluminescent images were acquired on a Kodak In-Vivo FX Imaging System (Carestream Molecular Imaging; Rochester, NY). Corresponding bright-field images were taken for anatomical reference of the bioluminescence signal. A series of spectra were acquired on tumor-bearing mice using the SpectroPen. First, the position of the SpectroPen was fixed to about 1−2 cm above the location of the acquisition area on

(34) Mishra, A.; Behera, R. K.; Behera, P. K.; Mishra, B. K.; Behera, G. B. *Chem. Rev.* **2000**, *100*, 1973–2012.

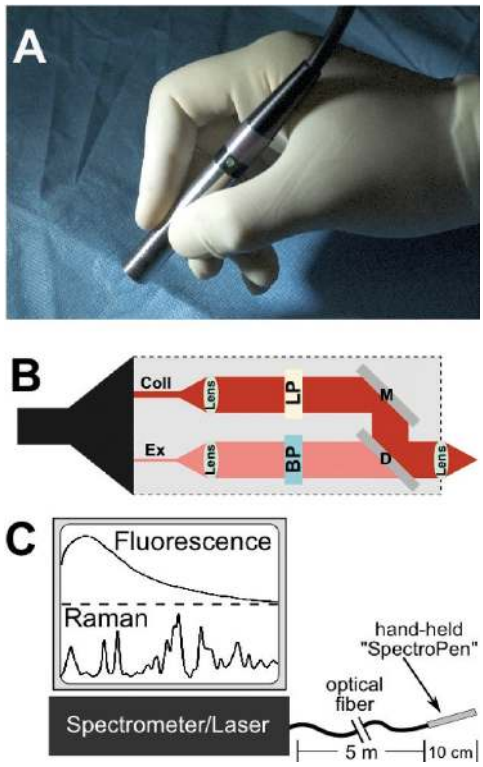

Figure 1. (A) Photograph showing the SpectroPen held in the operator's hand in a surgical setting. (B) Optical beam paths of the SpectroPen. Excitation light is provided from a 785 nm laser diode (200 mW output); Ex = excitation fiber, Coll = collection fiber, BP = band-pass filter, LP = long pass filter, *D* = dichroic filter, *M* = reflective mirror. (C) Schematic diagram of the complete system for wavelength-resolved fluorescence and Raman measurements. The spectra on the screen are actual fluorescence and SERS data obtained from 2 nM ICG and 20 pM gold nanoparticles (encoded with DTTC) with the SpectroPen and a desktop spectrometer (Advantage Series, DeltaNu).

the mouse. Spectra were collected in 1 s and were obtained from several locations, including directly over the center of the tumor and the peritumoral region. After the spectra were acquired, the integrated signal intensity was calculated. The signal intensity was compared to both the bright-field anatomical location and the bioluminescence signal.

RESULTS AND DISCUSSION

SpectroPen Design and Performance. The SpectroPen connects a hand-held sampling head, via a fiber optic cable, to a spectrometer that can record fluorescence and Raman signals (see Figure 1). The ability to resolve NIR fluorescent and Raman signals from background tissue arises from the optical filtering that takes place in the hand-held portion of the SpectroPen, as illustrated in Figure 1B. The laser light is transmitted through the excitation fiber into the pen. A first lens collimates the excitation light. Wavelength selectivity is provided by a band-pass filter. Excitation light is then focused onto the sample of interest. Back scattered light is collected through the same lens. A dichroic mirror and a long pass filter attenuate Rayleigh scattering by a factor of 10^8 in the collection fiber. Thus, only Stokes-shifted light is transmitted to the spectrometer. Silica Raman bands arising from the optical fibers are attenuated by physical filtering in both the excitation and emission optical paths. The

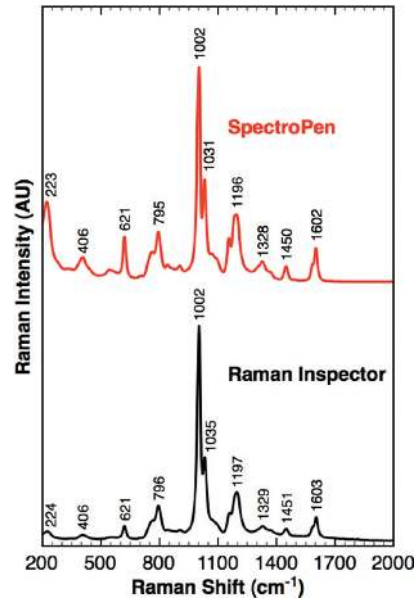

Figure 2. Raman spectra of a standard sample (polystyrene) obtained with the SpectroPen and a standard Raman spectrometer (Inspector by DeltaNu, Laramie, WY). This comparison shows that the SpectroPen's performance is similar to that of a conventional spectrometer in terms of signal-to-noise ratio, spectral resolution, and accuracy.

device's overall performance was evaluated by comparing the polystyrene Raman spectra obtained with the SpectroPen and a standard Raman spectrometer (see Figure 2). The results show well matched Raman signals between the two spectrometers and also with the literature spectra of polystyrene.[35] The differences in peak positions (wavenumbers) are less than 0.5% across the entire range of 200−2000 cm^{-1}. In general, the SpectroPen system performs as well as the standard Raman spectrometer as judged by signal-to-noise ratio, resolution, and wavelength accuracy.

Detection Sensitivity and Dynamic Range. As depicted in Figure 1C, the SpectroPen allows sensitive detection of both fluorescent and SERS contrast agents. A linear relationship is found between the recorded signal intensity and contrast agent concentration. Figure 3 shows the linear regression model fit to the integrated intensity versus concentration curves. Further examination shows a narrow 95% CI band (red dashed lines) indicating that the regression fit is very close to the "true" fit for both ICG and SERS contrast agents. The minimum spectrally resolvable concentrations (that is, limits of detection) are $2-5 \times 10^{-11}$ M for ICG and $0.5-1 \times 10^{-13}$ M for the SERS agent. It should be noted that the Raman reporter dye (diethylthiatricarbocyanine) used here is in resonance with the excitation wavelength at 785 nm, so the phenomenon should be correctly called surface-enhanced resonance Raman scattering (SERRS). It is also worth noting that the SERRS nanoparticles are 40−50 fold more sensitive than ICG under our experimental conditions, primarily because of the poor optical properties of ICG (less than 2% quantum yield and fluorescence quenching induced by aggregation). The maximum detectable concentration is determined by detector signal saturation, the analog-to-digital converter (16 bits, 2^{16} = 65 536), and the data

(35) Sloane, H. J.; Bramston, R. *Appl. Spectrosc.* **1973**, *27*, 217–225.

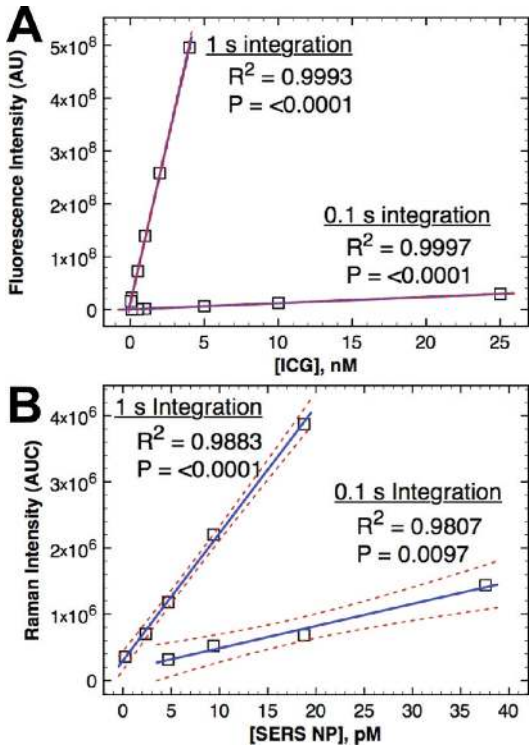

Figure 3. (A) Fluorescence and (B) Raman signals obtained with the SpectroPen at different contrast agent concentrations. The linear regression model is shown as a blue line with 95% confidence intervals shown as dashed red lines. R^2 is the fit coefficient of the linear regression model, and has a value of 1 for perfect fits. The *P*-values indicate that the slopes of the linear regression are significantly different than zero.

integration time. That is, for low contrast signals, the integration time should be increased in order to improve the signal-to-noise ratio, whereas for high contrast signals, the integration time should be reduced to avoid detector saturation (which will allow high-speed acquisition of tumor contrast signals). The dynamic range is then defined by the low and high limits in which the contrast signal intensity is linear with its concentration. For both fluorescence and Raman measurements, the SpectroPen provides a 50−60 fold dynamic range. This finding has significance because weak tumor-margin signals that are 50−60 fold lower than the central tumor signals can be measured simultaneously without adjusting the data acquisition parameters (see below).

Spectral Discrimination and Tissue Penetration Depth. The ultimate goal of intraoperative use of the SpectroPen is detection of tumor foci at the margins of the tumor mass, thereby minimizing the risk of positive margins. Such a real-time detection system would allow the surgeon to remove tumor tissue that might have gone undetected, saving the patient from repeated surgery and potentially improving survival. Sensitive tumor detection is based on the use of albumin-bound ICG or SERS nanoparticles as contrast agents. As discussed in more detail later, the main mechanism is believed to be "passive tumor targeting" in which nanoparticles are accumulated and retained in the tumor interstitial space mainly through the enhanced permeability and retention (EPR) effect.[36,37] First, we examined the ability of the SpectroPen

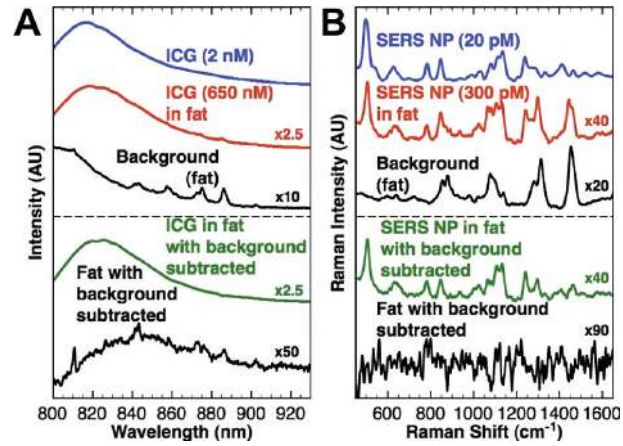

Figure 4. (A) Fluorescence spectra of pure ICG, animal fat, and a mixture of ICG and animal fat before background subtraction (upper) and after background subtraction (lower). (B) Raman spectra of pure SERS nanoparticles, animal fat, and a mixture of SERS nanoparticles and animal fat before background subtraction (upper) and after background subtraction (lower). All spectra were taken with the SpectroPen positioned 1-cm above the top layer of tissue. Spectra were acquired over 0.1−10 s. The background was obtained by averaging four different spectra obtained from control tissues, and was subtracted from the contrast-enhanced spectra or from single background measurements. Signal intensities relative to that of pure ICG or SERS samples are indicated by scaling factors. The Raman reporter dye was diethylthiatricarbocyanine (DTTC).

to differentiate contrast agent signals from the autofluorescence and Raman scattering of major tissue/organ types (i.e., fat, liver and lung). Figure 4A shows representative spectra of pure ICG, animal fat, and a mixture of ICG and animal fat (ICG in fat). At 785 nm excitation, ICG has a fluorescence peak at 816 nm, while fat has a background fluorescence peak at 805 nm plus resolvable Raman signals at 862, 1070, 1297, 1439, 1652 cm^{-1} (corresponding to 842, 857, 874, 885, and 902 nm in wavelength, respectively). ICG buried in fat has identifiable contributions of both ICG and fat (e.g., ICG fluorescence at 816 nm and the fat Raman peaks at 874 and 885 nm). As shown in Figure 4A (lower panel), the background signal of fat can be accurately subtracted, allowing nearly pure ICG contrast signals. Similarly, the data in Figure 4B (upper and lower panels) show that the background Raman spectrum can be subtracted to reveal predominantly the SERS contrast signals.

As noted earlier, the ability to detect deeper satellite residual tumors adjacent to the primary tumor is important to complete tumor resection and improving patient outcome. To simulate this surgical scenario, we examined the ability of the SpectroPen to detect optical contrast agents below the surface of fat, liver, and lung tissues by placing contrast agent loaded tissue specimens below 1−2 mm sections of unlabeled tissue (Figure 5A). Figure 5B and C shows the relationship between signal intensity and the depth of ICG or SERS agents deeply placed in ex vivo tissues. As expected from light scattering, the contrast signal intensity decreased almost exponentially with tissue thickness. It is worth noting that ICG can be detected more deeply in fat than other tissues because fat does not scatter the excitation light as strongly as lung and liver. This finding has potentially important applica-

(36) Li, S.-D.; Huang, L. *Mol. Pharm.* **2008**, *5*, 496–504.

(37) Smith, A. M.; Duan, H.; Mohs, A. M.; Nie, S. *Adv. Drug Delivery Rev.* **2008**, *60*, 1226–1240.

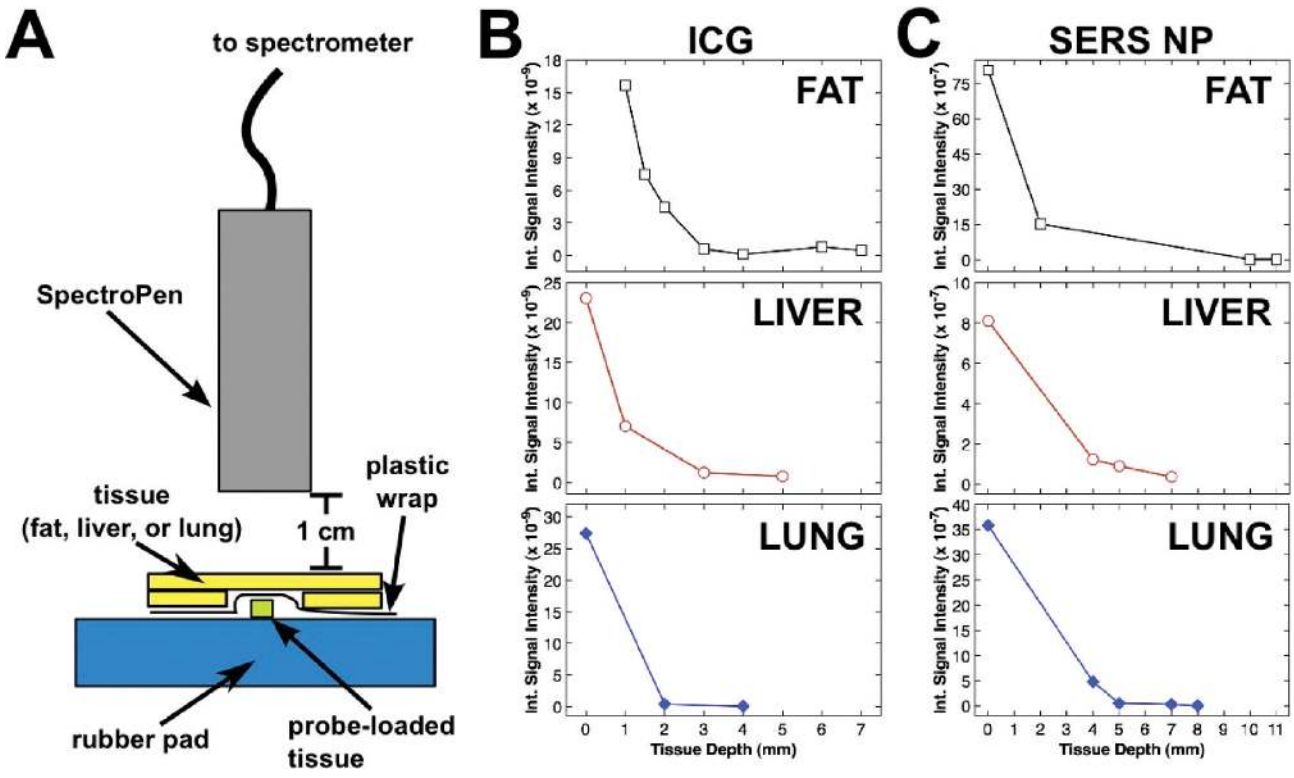

Figure 5. (A) Experimental setup for tissue penetration depth studies of near-infrared fluorescent and SERS contrast agents. (B) ICG and (C) SERS signals as a function of placement depth of contrast agents in fresh fat, liver, and lung tissue (see text for discussion). All spectra were recorded with the tip of the SpectroPen positioned at about 1 cm above the top layer of tissue and acquired over 0.1−10 s using diethylthiatricarbocyanine (DTTC) as the Raman reporter dye.

tions in lipomatous (fat-rich) tissues such as breast and some other soft tissues. In addition, lung and liver have more intense autofluorescence with NIR excitation (likely due to porphyrins and related chromophores in these highly vascularized organs), which compromises the ability to distinguish ICG emission from native autofluorescence. In comparison, SERS nanoparticles give rise to sharp spectral peaks that are distinct from the broad background, allowing accurate extraction of weak SERS signals under high-attenuation and scattering conditions. Thus, weaker SERS signals can be detected and resolved at a greater tissue depth in comparison with ICG fluorescence. The penetration depth can be further improved by positioning the fiberoptic tip closer to the tissue surface (almost in contact).

In Vivo and Intraoperative Tumor Detection. We have conducted in vivo investigations to test the ability of the SpectroPen to detect intratumoral deposition of ICG after intravenous infusion. This contrast agent has been approved by the U.S. Food and Drug Administration (FDA) and is indicated for various uses in humans such as determining cardiac output, hepatic function and liver blood flow, and for ophthalmic angiography.[38] To assess degree of tumor contrast enhancement using ICG, we used mice in whom 4T1 tumor cells (2×10^6 in number) were subcutaneously injected 18 days prior to imaging. The tumor cells were genetically engineered to express the firefly luciferase gene; intravenous injection of luciferin after tumor development causes these cells to emit bioluminescent light and allows one to determine the precise location of tumors using bioluminescence imaging. Thus, ICG contrast enhancement could be correlated with simultaneous bioluminescence imaging to determine whether ICG contrast enhancement (if any) originated from tumor sites. On day 17 after tumor cell inoculation, we intravenously infused ICG into the mice using a dose of 357 μg/kg, which is the equivalent dose used for human use, and then imaged the mice using the SpectroPen 24 h later. Using bioluminescence imaging, we identified a dominant tumor site and two satellite tumor sites along the track of the needle used for inoculation of tumor cells (Figure 6). We obtained a set of 14 spectra from the mouse using the SpectroPen. Figure 6 highlights the high degree of ICG contrast enhancement in the tumors compared to the surrounding tissues. The intense ICG signals at locations 5−9, 13, and 14 are indeed correlated with the presence of tumor as determined by bioluminescence. The integrated signal intensities from the tumor areas are nearly 10 times more intense than the signals obtained from normal regions. Spectra collected from the adjacent edges (less than 2 mm from the tumor) are still 5−6 times stronger than that of the more remote areas, providing excellent delineation of the tumor.

After surgical removal of the tumors, bioluminescence imaging shows that the excised tumors are bright and the surgical cavity

(38) Ott, P. *Pharmacol. Toxicol.* **1998**, *83*, 1–48.
(39) Parungo, C. P.; Colson, Y. L.; Kim, S. W.; Kim, S.; Cohn, L. H.; Bawendi, M. G.; Frangioni, J. V. *Chest* **2005**, *127*, 1799–1804.
(40) Parungo, C. P.; Ohnishi, S.; De Grand, A. M.; Laurence, R. G.; Soltesz, E. G.; Colson, Y. L.; Kang, P. M.; Mihaljevic, T.; Cohn, L. H.; Frangioni, J. V. *Ann. Surg. Oncol.* **2004**, *11*, 1085–1092.
(41) Sevick-Muraca, E. M.; Sharma, R.; Rasmussen, J. C.; Marshall, M. V.; Wendt, J. A.; Pham, H. Q.; Bonefas, E.; Houston, J. P.; Sampath, L.; Adams, K. E.; Blanchard, D. K.; Fisher, R. E.; Chiang, S. B.; Elledge, R.; Mawad, M. E. *Radiology* **2008**, *246*, 734–741.
(42) Yamashita, S. I.; Tokuishi, K.; Anami, K.; Miyawaki, M.; Moroga, T.; Kamei, M.; Suehiro, S.; Ono, K.; Takeno, S.; Chujo, M. *J. Thorac. Cardiovasc. Surg* **2010**, in press.

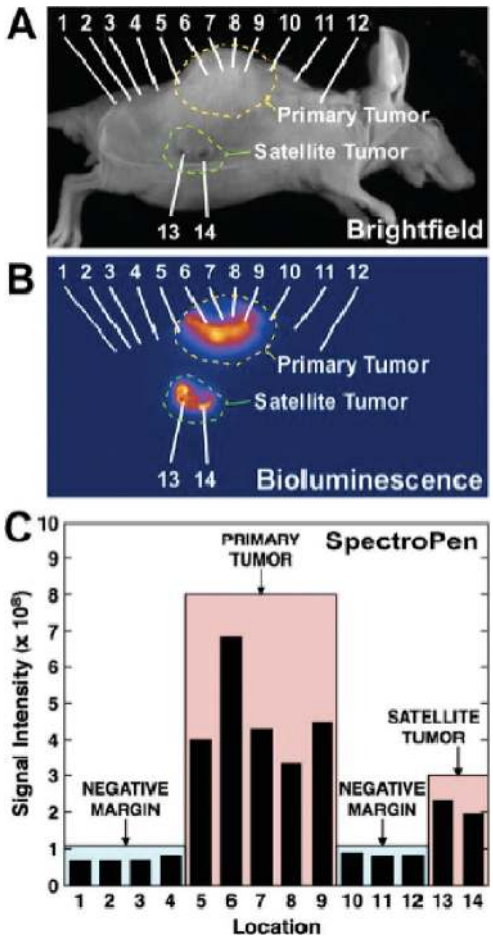

Figure 6. (A) Bright-field image showing the anatomical locations of a primary 4T1 breast tumor and two satellite nodules (dashed circles). The specific locations for SpectroPen measurement are indicated by numbers 1−12 for the primary tumor and 13−14 for the satellite nodules. (B) Bioluminescence image of the mouse showing the primary and satellite tumors (red signals). (C) Integrated ICG signal intensities as recorded by the SpectroPen at various locations corresponding to the numbers in (A) and (B).

is dark (see Figure 7). Spectra recorded by the SpectroPen indicate 10-fold stronger signals for the excised tumors compared to the cavity, which is consistent with the contrast ratio of tumor to healthy tissue found within the living animal (Figure 6). Interestingly, there was a very small area of bioluminescence remaining at the margin of the cavity, corresponding to a positive surgical margin, that was not seen by visual inspection alone. Reexamination of this area with the SpectroPen revealed an ICG signal that was 5 times stronger that adjacent tissue, again consistent with the contrast ratios recorded from noninvasive imaging. The ability to obtain a strong ICG signal from tumor, remove the tumor as guided by the SpectroPen, and obtain real-time pathology about the margin status of both excised tissue and the remaining tumor cavity, are all important features for image-guided surgery.

One notable feature of our SpectroPen results is that the observed ICG contrast between tumor and normal tissues is very clear and strong, even though no tumor-targeting ligands are used in this work. Previous oncology studies utilizing ICG are mainly directed toward sentinel lymph node detection.[39−42] These studies rely on direct intratumoral or peritumoral injections of ICG rather than the intravenous route of administration used in our study. After intravenous administration, ICG is known to bind to the hydrophobic pockets of serum proteins, especially albumin and lipoproteins.[38] Thus, through protein binding, ICG takes on nanometer scale dimensions, with a hydrodynamic size of 6−8 nm diameter. The strong tumor enhancement comes from the enhanced permeability and retention (EPR) effect,[43] in which macromolecules or nanoparticles preferentially accumulate in tumor due to the abnormal neovasculature with large fenestrations and poor lymphatic drainage characteristic of tumors. More advanced nanoparticle formulations of ICG have been reported to facilitate longer circulation of ICG and increased tumor accumulation for diagnostic and photothermal applications.[44−47] Also, targeted contrast agents can be developed by conjugating SERS and other nanoparticles to peptides, monoclonal antibodies,

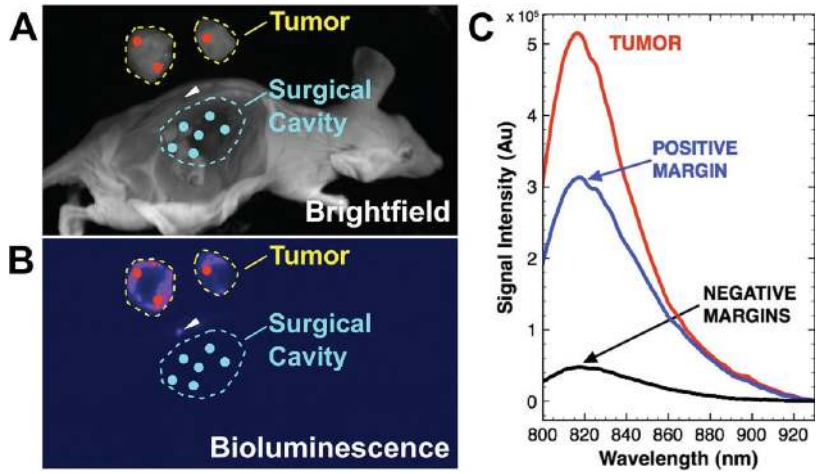

Figure 7. Detection of positive and negative tumor margins by using the SpectroPen. (A) Bright-field and (B) bioluminescent images showing the resected tumor (yellow dashed lines) and the surgical cavity (cyan dashed line). Spectra obtained within excised tumor are shown in red, those in the surgical cavity are shown in cyan, and one on the margin of the surgical cavity is shown by a white arrowhead. As seen on the bioluminescence image, there was a region with residual tumor along the margin of the cavity. This region was detected by the SpectroPen by its signal intensity much greater than background. (C) Averaged spectra from the tumors and positive and negative margins. Overall, the cavity showed minimal fluorescence emission and had 10-fold lower emission than tumor tissue.

and small-molecule ligands for molecular recognition of antigens or receptors on the surface of tumor cells.[48]

In summary, we have developed a hand-held spectroscopic device and have demonstrated the use of two near-infrared contrast agents for in vivo and intraoperative tumor detection. Under in vitro conditions, the hand-held device provides a detection limit of $2-5 \times 10^{-11}$ M for ICG and a detection limit of $0.5-1 \times 10^{-13}$ M for SERS. The tissue penetration depth is about 5−10 mm depending on the tissue's optical properties and the ability to resolve weak contrast signals. We have also carried out in vivo studies by using mouse models bearing bioluminescent 4T1 breast tumors. The results show that the tumor borders could be precisely detected preoperatively and intraoperatively, resulting in real-time detection of both positive and negative tumor margins around the surgical cavity. In comparing the two types of near-infrared contrast agents, SERS nanoparticles (60−80 nm) provide rich spectroscopic information (sharp spectral features), but are much larger than the ICG-albumin complexes (4−6 nm). So the SERS agent is likely better suited for mapping blood vessels and tumor boundaries/peripheries (important for delineating tumor margins), whereas ICG-albumin should be better for tumor penetration and rapid clearance.

(43) Matsumura, Y.; Maeda, H. *Cancer Res.* **1986**, *46*, 6387–6392.
(44) Barth, B. M.; Sharma, R.; Altinoğlu, E. I.; Morgan, T. T.; Shanmugavelandy, S. S.; Kaiser, J. M.; McGovern, C.; Matters, G. L.; Smith, J. P.; Kester, M.; Adair, J. H. *ACS Nano* **2010**, *4*, 1279–1287.
(45) Saxena, V.; Sadoqi, M.; Shao, J. *Int. J. Pharm.* **2006**, *308*, 200–204.
(46) Saxena, V.; Sadoqi, M.; Shao, J. *J. Photochem. Photobiol., B* **2004**, *74*, 29–38.
(47) Yaseen, M. A.; Yu, J.; Jung, B.; Wong, M. S.; Anvari, B. *Mol. Pharm.* **2009**, *6*, 1321–1332.
(48) Singhal, S.; Nie, S.; Wang, M. D. *Annu. Rev. Med.* **2010**, *61*, 359–373.

ACKNOWLEDGMENT

A.M.M. and M.C.M. contributed equally to this work. We are grateful to Dr. Keith Carron and Mr. Matt Russell (DeltaNu, Laramie, WY) for help in device design and development, to Professor Ximei Qian (Emory University) for surface-enhanced Raman scattering studies, and to Professor Lily Yang (Emory University) for providing the bioluminescent 4T1 cancer cell line. This work was supported in part by grants from the Centers of Cancer Nanotechnology Excellence (CCNE) Program (U54 CA119338) and the U.S. National Institutes of Health Grand Opportunity (GO) grant (RC2 CA148265). M.D.W., B.L.J., and S.N. are Distinguished Scholars of the Georgia Cancer Coalition (GCC). A.M.M. acknowledges the NCI Nano-Alliance Program for a Pathway to Independence Award (K99CA153916).

Received for review August 3, 2010. Accepted September 16, 2010.

AC102058K